

PRINCIPAL POINT BEHAVIOUR AND CALIBRATION PARAMETER MODELS FOR KODAK DCS CAMERAS

By M. R. SHORTIS,
University of Melbourne

S. ROBSON*
University College London

and H. A. BEYER
Imetric SA, Switzerland

(Based upon a paper read by the first author at a Technical Meeting of the
Photogrammetric Society on 11th November, 1996)

Abstract

Digital still cameras have been widely adopted for close range photogrammetry and machine vision applications. Due to the advantages of onboard storage of digital images, portability and rapid data processing, digital still cameras are rapidly becoming standard equipment for measurement tasks such as industrial metrology and heritage recording. As for any metric application, the accuracy of the derived object data is dependent, amongst many other factors, on the accuracy of the camera calibration. For the vast majority of photogrammetric applications, use of the simple case of a block invariant calibration model comprising the primary physical parameters, including the principal point position, is sufficient. However, cameras designed for photojournalism and domestic use, such as the Kodak DCS420 and 460 cameras, are well known for their calibration instability because the design is based on a 35 mm SLR camera body. In particular, previous research has shown that the principal point location is prone to movement during normal handling of the camera, due to the mounting mechanism of the CCD array. This paper reports on an investigation of the physical behaviour of the principal point location and compares different calibration parameter models for the Kodak DCS420 and DCS460 digital still cameras.

KEY WORDS: principal point, camera calibration, digital camera

*Formerly at City University, London.

FRONTISPIECE. A unique remote application of digital photogrammetry used as an inspection tool during the first fully remote shutdown at JET Joint Undertaking, the European Union fusion research project based at Culham, Oxfordshire, England. An article by Macklin *et al.* describes the work elsewhere in this issue of the *Photogrammetric Record*.

INTRODUCTION

DIGITAL STILL CAMERAS have gained wide acceptance for high precision optical three dimensional measurement, particularly in the application areas of industrial inspection and large scale metrology in manufacturing and engineering (Beyer, 1995). Digital still cameras are now a fundamental component of vision metrology systems (Fraser, 1997), used either as a single roving camera (offline mode) or in multiple camera configurations as part of a work cell arrangement (online mode). The acceptance of these cameras is based principally on the efficiency with which they can be used and the accuracy levels which can be achieved. The cornerstone of their efficiency is the use of digital images, which can be rapidly acquired and processed. In particular, advances in the automation of vision metrology systems (Fraser, 1997) would not be feasible without the use of cameras which capture digital still or video-rate images.

A digital still image camera which has proved to be extremely popular for metric applications is the Kodak DCS series (Susstrunk and Holm, 1995; Peipe, 1995). This camera series is designed essentially for photojournalism, but has many desirable features for a digital image photogrammetric camera. The high resolution of the CCD sensor, combined with high image storage capacity and ready availability, has made the DCS the common choice for vision metrology applications where system portability is important. Although there are other digital still cameras with similar features (Shortis and Beyer, 1996; Maas and Neideröst, 1997; Peipe, 1997), the DCS series is certainly the most widely used camera for industrial inspection and large scale metrology. The DCS series has also found acceptance for other applications, such as architectural recording (Streilein and Gaschen, 1994), surface reconstruction (Petran *et al.*, 1996) and low altitude mapping (Mills *et al.*, 1996).

The accuracy of vision metrology systems based on digital still cameras is dependent on the image resolution, image scale, image measurement precision and a number of other factors, such as network design (Fraser and Shortis, 1995). The principal influence on accuracy for the DCS series is the resolution of the CCD sensor. Utilizing a 1536×1024 element CCD array, the DCS420 and its predecessors are widely used for measurement tasks which require relative precisions in the range 1:50 000 to 1:80 000 (Fraser and Shortis, 1995). (Relative precision is the ratio of the mean target co-ordinate precision, as derived from the photogrammetric network solution, to the largest span of the target array.) Relative precisions well in excess of 1:100 000 (Peipe, 1995) can be achieved with the DCS460, which has an image resolution of 3096×2048 pixels. These levels of precision presuppose high contrast targeted points in the object space and image measurement using centroids, template matching or ellipse fitting (Luhmann, 1996). The level of precision can be improved by using multiple exposures at each camera station in a network (Fraser and Shortis, 1995), which can be readily carried out using the high image capacity of the DCS series.

Like any camera used for metric applications, calibration is necessary for digital still cameras because systematic errors in the collinearity condition must be modelled or eliminated. Both the offline and online modes of operation typically adopt self calibration at a single focus setting, with the camera lens locked in position to minimize variation in principal distance and other focus dependent parameters of interior orientation. In general, a block invariant additional parameter model is employed, which assumes that there is no change in the interior orientation of the digital still camera between exposures. As a consequence, reported image space precisions are typically of the order of $1/50$ to $1/30$ of a pixel, or $0.2 \mu\text{m}$ to $0.3 \mu\text{m}$.

Rigorous independent checks of object space accuracy, where available, can show degradations of the order of 100 per cent when compared to internal measures

of precision (Shortis *et al.*, 1995; Fraser and Shortis, 1995). In other words, relative accuracy is typically poorer than relative precision. (Relative accuracy is the ratio of the target co-ordinate r.m.s. error to the largest span of the target array, where the r.m.s. error is computed from co-ordinate differences with respect to the independent determination of target co-ordinates after a three dimensional similarity transformation between the two co-ordinate sets.) There are many potential sources of systematic error which may contribute to the disparity between relative accuracy and relative precision. The primary potential sources which have been identified are calibration stability (Shortis and Beyer, 1997), variation of distortion (Fraser and Shortis, 1992; Shortis *et al.*, 1996), unflatness of the CCD array (Fraser *et al.*, 1995), perspective distortion of targets (Dold, 1996) and optical aberrations (Robson and Shortis, 1998), to name just a few. This paper investigates the specific issues of calibration stability and behaviour of the principal point location for Kodak DCS series cameras.

CALIBRATION STABILITY

There are a number of factors which affect the calibration stability of the Kodak DCS camera series. Cameras based on the 35 mm SLR body are well known for their lack of robustness (Fryer, 1985). The lack of robustness of this camera type is a combination of body instability and film unflatness variability, of which the former will certainly have an effect on the Kodak DCS type. A further complication is that the camera body to digital back mounting is not rigid, as the camera body is only partially constrained (Fig. 1). Previous research has shown that stabilization of the camera body with respect to the digital back is effective in increasing stability (Shortis and Beyer, 1997), indicating that the non-rigid mounting is a factor in the calibration stability.

An additional factor is that the CCD sensor is spring mounted to minimize the effects of shock from mishandling of the camera. The flexibility of the CCD array mounting has direct consequences for the fidelity of the collinearity solution, because the CCD array defines the focal plane and this is generally assumed to be fixed with

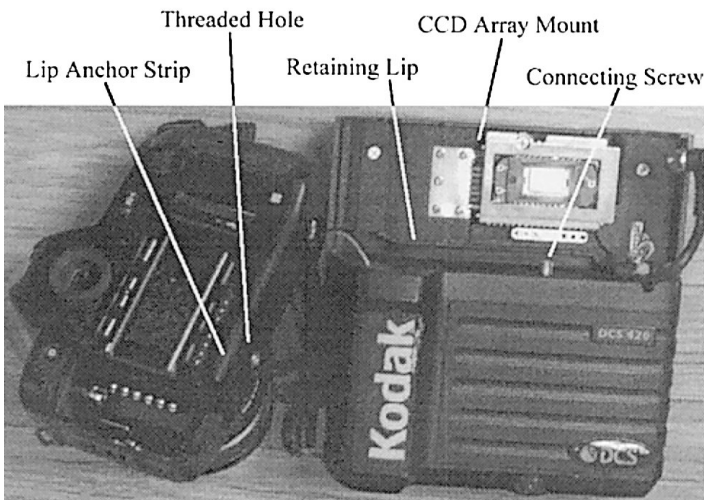


FIG. 1. Camera body to digital back connexion and CCD array mounting of the Kodak DCS420.

respect to the perspective centre of the objective lens. Disassembly of a DCS shows clearly that the CCD array can rotate in the vertical direction (camera held upright) with respect to the electrical connexions which are fixed to the camera back (Fig. 1). A lesser amount of movement is possible in the horizontal direction. Both of these possible movements are nominally within the focal plane of the camera. Movement in the direction perpendicular to the focal plane, parallel to the optical axis, is only possible whilst the camera is disassembled, as markings on the CCD array surround indicate that the array is pressed against the digital back when the camera is assembled for operation.

If the camera is rotated about a horizontal optical axis, the effect of gravity will result in rotational and lateral responses from the CCD array, unless it is pressed very firmly against the camera back. Inspection of a relatively small sample of cameras indicates that in general the pressure is light, as the markings on the CCD array surround are often ill-defined or smeared. The amount of potential movement is governed by the pressure imposed on the CCD array by the camera body. It could be expected that variations in pressure, due to variations in the quality of manufacture and assembly, are likely to lead to significant variations in CCD array movement. If several cameras are investigated over a sufficiently long period of time, the magnitude of any movements could be expected to be different for both different cameras and at different epochs for the same cameras. Hence, if the focal plane is moving, the location of the principal point (PP) will appear to move with respect to a constant frame of reference on the CCD array.

There is substantial evidence for variability in PP position and perhaps other parameters for the DCS during offline use (Gruen *et al.*, 1995), particularly when offline use is contrasted with online use (Shortis and Beyer, 1997). The variations detected for offline use are caused by the handling of the camera during operation and the orthogonal roll strategies used to minimize parameter correlations in self calibrating networks (Kenefick *et al.*, 1972). In contrast, online use does not involve handling of the camera nor roll strategies, because the camera is fixed on a tripod or other support. There is some evidence that, given a consistent focus, lens distortion is stable in the medium to long term (Shortis and Beyer, 1997), indicating that the variation in the focal plane location with respect to the lens is the principal source of calibration instability.

A thorough analysis of the stability of the camera requires all aspects of camera calibration to be considered. The analysis in this investigation concerns only the PP variability in order to characterize behaviour and derive appropriate parameter models. The assumption is that the main influence on PP movement is camera roll, due to the mechanism by which the CCD array is mounted in the camera. Although other influences may be present, such as camera body flex, these effects are assumed to be of a lesser importance and are unlikely to have the same consistency as the effect of roll.

In order to test the premise of poor physical robustness of the DCS camera, one option is stabilization of the CCD array and the camera body, as previously tested in the context of offline versus online stability (Shortis and Beyer, 1997). The effect of stabilization should be evident in a reduction in PP movement, or at least a change in the characteristic behaviour of the PP movement.

CALIBRATION MODELLING

Calibration models used in conjunction with the principle of collinearity are typically based on a mixture of primary physical terms and additional empirical terms which model the systematic errors in the perspective projection. Despite the mix of

TABLE I. Block invariant additional parameter model based on physical terms.

<i>Parameter name</i>	<i>Parameters and/or model</i>
Position of the principal point	x_p, y_p
Principal distance	pd
Radial lens distortion	$\Delta r = k_1 r^3 + k_2 r^5 + k_3 r^7 + \dots$
Decentering lens distortion	$\Delta x = p_1(r^2 + 2x^2) + p_2(2xy)$
	$\Delta y = p_1(2xy) + p_2(r^2 + 2y^2)$
Orthogonality and affinity	$\Delta x = a_1 x + a_2 y$

x, y = image co-ordinates with respect to the principal point; and
 r = radial distance with respect to the principal point.

physical and additional terms, the calibration model is commonly known as an additional parameter model. The most widely used block invariant additional parameter model based on physical terms (Fryer, 1996) is shown in Table I.

The additional parameter model is adopted as block invariant when it applies to every image in a network. The implication of this adoption is that the camera has a stable calibration and is used at a constant focus. Multiple cameras (Fraser *et al.*, 1995) or a single camera with multiple focus settings (Shortis *et al.*, 1996) may be used, but each instance has an associated block invariant parameter set. In order to provide a comparison with a "standard" model, the block invariant additional parameter model is used in this investigation as a base line against which other models are tested.

The alternative to a block invariant parameter set is a partial or fully photo-invariant parameter set. A fully photo-invariant parameter set implies that every exposure in a network has a separate set of calibration parameters. This is an implausible scenario because a totally unstable camera is unlikely to be used for precise applications and, as is discussed later, such a network would be inherently weak. A much more applicable scenario is a partial photo-invariant parameter set where some parameters are constant for the full network, whilst others are photo-invariant and apply to individual exposures (Fraser, 1987).

Under the assumptions that the CCD array is adequately pressed against the digital back, that body flex and instabilities in the lens mounting system have an insignificant effect, and that the lens focus is unaltered within a single network, the principal distance can be adopted as a block invariant parameter applied to all photographs. Undue body flex or array movement would result in a defocusing of the image, which from experience and anecdotal evidence is not apparent for these cameras. As previously noted, evidence from other research on medium term calibration stability (Shortis and Beyer, 1997) indicates that lens distortions, given that the lens focus is unchanged, are stable and can also be incorporated as block invariant parameters. The orthogonality and affinity terms are generally insignificant for the DCS camera (Shortis and Beyer, 1997) and other research has indicated that they are a function of the lens optics rather than the CCD sensor (Fraser *et al.*, 1995). Again, assuming a constant focus for the lens, these terms can be adopted as block invariant.

If the justification for the block invariance of the other parameters is accepted, then only the PP parameters are adopted as photo-invariant. This is in accord with the proposition that the CCD is moving with respect to the lens optical axis because of handling during operation and the roll strategy employed during the image acquisition for a network. Although out of plane rotation cannot be ruled out entirely, it is assumed here that the major component of movement is within the plane of the CCD array and therefore within the focal plane.

In each of the three following cases of variable PP calibration models, the other

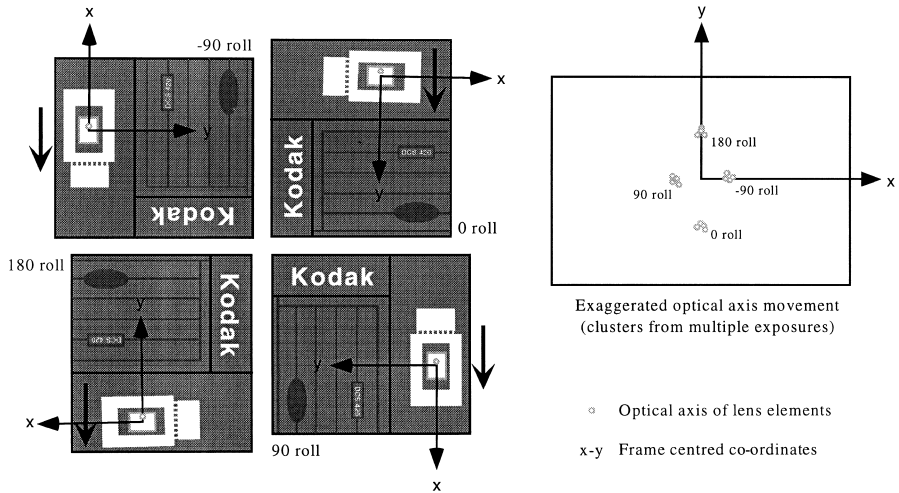


FIG. 2. Expected motion of the CCD array and interpreted PP movement.

physical parameters already described are considered to be block invariant, whilst the PP calibration parameters vary for each and every exposure.

The most comprehensive model for CCD array movement is independent photo-invariant PP parameters, where every image has an associated pair of PP location parameters. This is a logical consequence of the typical geometry of self-calibrating networks, which have different roll angles for every photograph. Therefore it could be expected that there would be a different PP location for every photograph. However, some weakening of the network is inevitable, because the PP parameters for each photograph are determined from the image observations on that photograph only and there will be a reduction in the overall number of redundancies in the network due to the increase in the number of unknown parameters. In order to reduce the number of calibration parameters, and therefore reduce the weakening of the self-calibrating networks, other calibration models for the PP location can be considered. The response of the PP location to roll angle may be physically modelled by a pseudo-circular motion function (Fig. 2). It could be expected that the magnitude of the movement will be greater in the *y* axis direction for the CCD array, because the rotational motion is greater than the possible movement against the electrical connector. Therefore, in an ideal case, an elliptical pattern of movement might be expected in response to a continuous rolling action. This leads to a PP parameter model which has constant components related to the expected magnitude of movement and a variable component which is dependent on camera roll, as follows:

$$x_p = x_0 - r_x \sin(\text{roll})$$

$$y_p = y_0 - r_y \cos(\text{roll}),$$

where *r* is a “radius” of motion for each component and it is assumed that the effect on the *y* component will be maximized in the upright and upside down orientations and minimized in the left and right roll orientations, with the opposite effect on the *x* component

An additional complication for the elliptical motion model is that it could be expected that the tilt of the camera would influence the degree of PP movement. In

TABLE II. Principal point parameters grouped with sectors of orthogonal roll angles.

Group	Roll angle range
1	$-45^\circ \leq \text{roll} < 45^\circ$
2	$45^\circ \leq \text{roll} < 135^\circ$
3	$135^\circ \leq \text{roll} < -135^\circ$
4	$-135^\circ \leq \text{roll} < -45^\circ$

the extreme case of a vertical photograph with the CCD array in the horizontal plane, little or no movement could be expected regardless of the roll angle employed. This leads to a slightly more complex pair of equations for the model as follows:

$$x_p = x_0 - r_x \sin(\text{roll}) \cos(\text{tilt})$$

$$y_p = y_0 - r_y \cos(\text{roll}) \cos(\text{tilt}),$$

which assume that the maximum effect is encountered when the optical axis of the camera is horizontal, the plane of the CCD array is vertical and the corresponding tilt is zero. These equations are somewhat empirical, but they do reflect the expected physical movement of the CCD array.

The third model proposed is purely empirical, based on the typical roll strategy used in self calibrating networks. The orthogonal roll angles used in self calibrating networks tend to be oriented on the cardinal directions of 0° , 90° , 180° and -90° , as they correspond to upright, left roll, upside down and right roll respectively. Therefore, a grouping of PP parameters with sectors of orthogonal roll angles is feasible, as shown in Table II.

Clearly this is not a universal solution, because two photographs with close to 45° of roll angle, which would be expected to have similar PP locations, may fall into different groups and therefore would not share the same PP parameters. However, this partial block invariant additional parameter model does have application to networks with a rigorous cardinal direction roll strategy.

Neither the elliptical motion nor roll grouping models will be efficient if the CCD array does not show a reasonable degree of hysteresis. In other words, it is assumed that the roll effect is very systematic and the CCD array will return to the same physical position given the same approximate roll angle.

EXPERIMENTAL WORK

The majority of the camera calibration data used for the analysis of PP behaviour is drawn from a programme of experiments investigating calibration stability (Shortis and Beyer, 1997) and variation of distortion with focus and within the depth of field (Shortis *et al.*, 1996). In addition, some data sets were opportunistically used, based on one off calibrations of cameras. These data were gathered at Imetric SA during 1996, where three DCS460 and three DCS420 cameras were calibrated with various roll schemes. Additional data were subsequently gathered at the University of Melbourne, where a fourth DCS420 camera and two Leica/GSI INCA 4.2 cameras were calibrated. This later test at the University of Melbourne incorporated an accuracy evaluation, which was not conducted at Imetric. The 18 different cases are shown in Table III.

The processing of all 18 cases employed self calibration, free networks and a targeted test range approach. Either *ad hoc* target field arrangements or purpose built

TABLE III. Details of the 18 calibration data sets used in the experimental testing.

Case	Camera	Target array type	Lens (mm)	Number of images	Number of targets	Roll scheme
1	DCS460-1	Cross and rods	20	12	100	Random
2	DCS460-2	Cross and rods	20	32	100	Random
3	DCS460-2	Calibration field	18	20	140	Dual-roll
4	DCS460-2	Calibration field	24	24	140	Dual-roll
5	DCS460-2	Calibration field	24	32	140	Quad-roll
6	DCS460-2	Calibration field	20	32	140	Quad-roll shaken
7	DCS460-2	Calibration field	24	32	140	Quad-roll consistent
8	DCS460-2	Calibration field	18	32	140	Quad-roll consistent
9	DCS460-3	Calibration field	20	24	140	Tri-roll consistent
10	DCS420-1	Calibration field	18	32	90	Quad-roll
11	DCS420-1	Calibration field	14	32	90	Quad-roll
12	DCS420-1	Calibration field	14	32	90	Quad-roll consistent
13	DCS420-2	Calibration field	14	32	90	Quad-roll
14	DCS420-2	Calibration field	14	46	90	Quad-roll consistent
15	DCS420-3	Cross and rods	18	24	60	Random
16	DCS420-M	Calibration field	20	32	190	Quad-roll
17	INCA 4.2-1	Calibration field	17	32	190	Quad-roll
18	INCA 4.2-2	Calibration field	17	32	190	Quad-roll

test arrays were used. The *ad hoc* target arrays used at Imetric were typically made up from a carbon fibre orientation cross and a number of carbon fibre rods laid out on the floor with a total of either 60 or 100 targets (Fig. 3).

Calibrations using the *ad hoc* target field typically used a central camera station vertically above the centre of the array at which four photographs with orthogonal rolls were exposed, plus a number of camera stations around the periphery of the target array with convergent photography toward the centre of the target array. The photographs at the peripheral camera stations were typically exposed with a random roll strategy, which incorporated a mixture of cardinal roll directions and a variety of other orientations chosen to fill the frame of the camera.

The purpose built array at Imetric comprises 80 targets on a planar wall with the addition of approximately 65 targets on carbon fibre rods placed in the foreground. The purpose built array at the University of Melbourne is similar, comprising 135

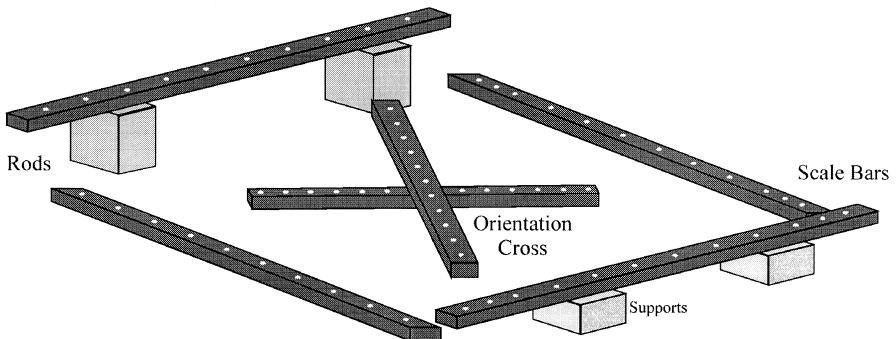


FIG. 3. Typical *ad hoc* target array used for calibrations.

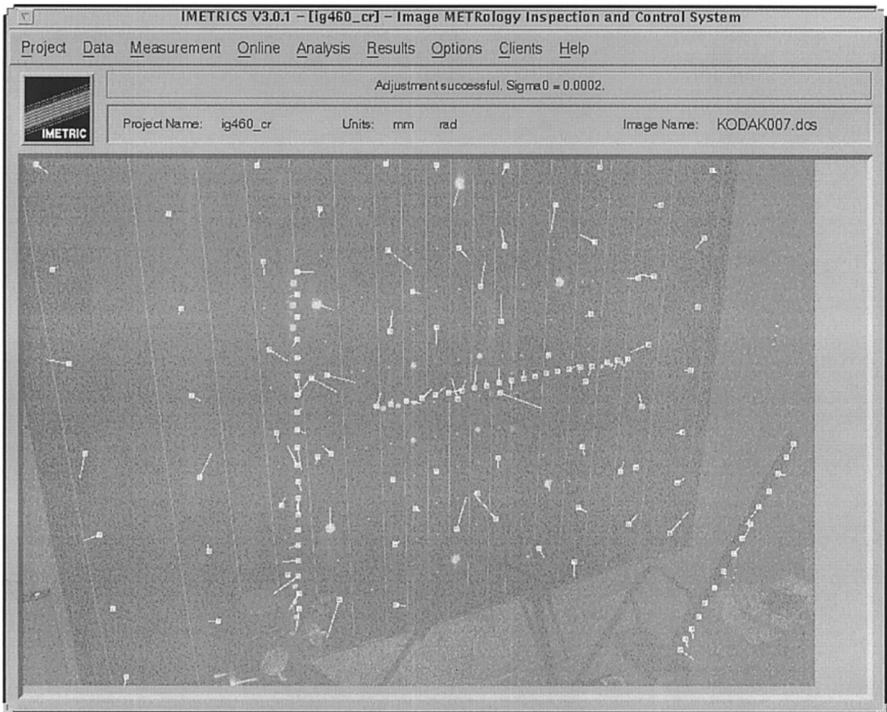


FIG. 4. Purpose built calibration field at Imetric SA. The graphic overlay indicates active target images and image co-ordinate residuals from the network solution.

targets on a planar wall and 55 targets in the foreground on a number of different fixtures. A typical layout of the target arrays is shown in Fig. 4, with a pseudo-regular grid of points on the wall and various fixtures in the foreground to provide an adequate third dimension. Although the planar array plus movable fixtures is a less than an ideal case, it is convenient as the requirement for permanent physical space in a laboratory is minimized.

Calibrations using the purpose built test array employed a network of between six and nine camera stations with convergent photography. Dual (0° and 90° rolls) or quadruple (0° , 90° , 180° and -90°) roll strategies were used at each station to simulate the typical practice in industrial metrology for minimization of parameter correlations. Typical practice also decrees, for the sake of efficiency, that each camera station is visited only once and two or four exposures are taken. Between each roll the camera is moved slightly to randomize the location and therefore randomize any systematic dependencies on station position (Fraser and Shortis, 1995).

In a number of cases, the camera stations within a single calibration network were visited three or four times with the camera held in a consistent orientation. This is in deliberate contrast to the normal operating mode of visiting each camera station only once and rolling the camera to each orientation at the camera station. The intent was to ascertain whether the CCD array would maintain a stable position if the camera was held in a constant attitude to the direction of gravity. Such a consistent

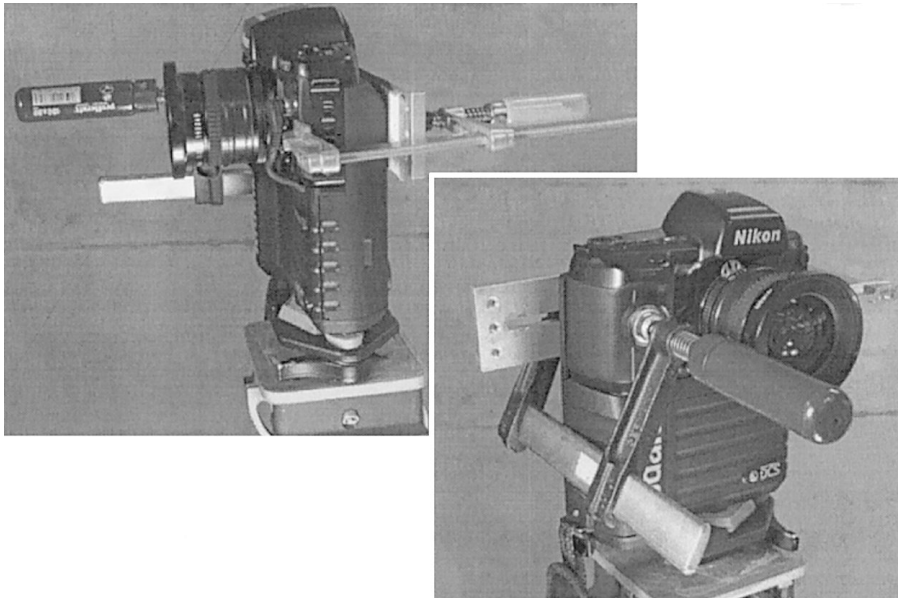


FIG. 5. The stabilized Kodak DCS420 camera.

roll strategy would be very inefficient, if not impractical, in real industrial metrology applications.

A DCS420 camera was modified by clamping the camera body to the digital back and fixing one corner of the CCD array (Fig. 5). This modification was intended to stabilize the camera and, particularly, the CCD array, in order to minimize the movement of the PP location (Shortis and Beyer, 1997). The solution was not intended to be absolutely comprehensive, as the CCD array must be given some freedom of movement to avoid shock damage in the case of a sudden impact on the camera. Furthermore, like the consistent roll strategy, this was not intended to be a practical solution for routine use of the DCS series of cameras, but instead was an attempt to verify the physical source of the camera instability.

In every case except the University of Melbourne DCS420 and INCA 4.2 cameras, the target images were measured by least squares template matching using the commercial Imetric software suite. In the case of the University of Melbourne cameras, the target images were measured by intensity weighted centroids (Trinder, 1989) using the VMS software suite, a digital image processing package developed jointly by two of the authors as a research tool. Again with the exception of the University of Melbourne data, the processing of the photographs was largely automated, using a combination of coded targets and image searching using multiphotograph epipolar matching. The efficiency and rapidity with which the close range networks could be measured and processed using this software allowed multiple calibrations to be carried out quickly, as well as enabling the use of *ad hoc* target arrays and foreground fixtures. The VMS software suite is not yet so advanced and a minor proportion of manual processing was necessary for the University of Melbourne data.

PHOTO-INVARIANT VERSUS BLOCK INVARIANT

The independent photo-invariant PP additional parameter model allows the PP co-ordinates to be adjusted for individual exposures. This model should realize the maximum level of improvement in internal consistency of the networks if the CCD array is moving with respect to the optical axis of the lens. The results of the network solutions for the block invariant and photo-invariant parameter models for the 18 cases are shown in Table IV. R.m.s. image residuals, maximum image residuals and estimates of unit weight are shown as the measures of internal consistency for the networks.

Estimates of unit weight are shown only for the first 15 cases in Table IV because these were computed using the Imetric software. In these cases, the target image locations were measured using template matching, which has the collateral benefit of providing an a priori estimate of the image measurement precision. It is

TABLE IV. Results for the 18 calibration data sets used in the experimental testing.

<i>Case and camera</i>	<i>Additional parameter model</i>	<i>R.m.s. image error (μm)</i>	<i>Maximum image error (μm)</i>	<i>Estimate of unit weight</i>	<i>Estimated relative precision</i>	<i>Mean 99% limit of PP values (μm)</i>	<i>Mean span of PP locations (μm)</i>
1	Block-inv	0.28	1.65	1.36	1:217 000	2.4	—
460-1	Photo-inv	0.24	1.14	1.17	1:228 000	6.0	15.2
2	Block-inv	0.43	3.25	3.19	1:268 000	2.0	—
460-2	Photo-inv	0.20	2.80	2.23	1:271 000	9.4	41.6
3	Block-inv	0.44	3.25	1.96	1:183 000	3.9	—
460-2	Photo-inv	0.20	2.80	0.98	1:359 000	3.1	30.0
4	Block-inv	0.31	2.19	1.11	1:305 000	3.9	—
460-2	Photo-inv	0.23	2.46	0.86	1:360 000	4.9	25.0
5	Block-inv	0.39	2.88	1.47	1:279 000	1.7	—
460-2	Photo-inv	0.25	2.69	0.95	1:360 000	4.6	34.7
6	Block-inv	0.76	6.42	3.09	1:138 000	2.7	—
460-2	Photo-inv	0.29	2.30	1.15	1:333 000	4.0	63.3
7	Block-inv	0.40	2.30	1.50	1:265 000	2.3	—
460-2	Photo-inv	0.25	1.84	0.93	1:359 000	4.2	31.7
8	Block-inv	0.70	4.07	3.33	1:149 000	2.0	—
460-2	Photo-inv	0.24	2.33	1.14	1:397 000	2.7	62.9
9	Block-inv	0.55	4.94	2.13	1:186 000	2.6	—
460-3	Photo-inv	0.29	3.10	1.18	1:292 000	5.0	62.9
10	Block-inv	0.22	1.04	1.21	1:256 000	3.3	—
420-1	Photo-inv	0.17	0.87	0.89	1:298 000	7.5	29.6
11	Block-inv	0.25	1.33	1.25	1:226 000	1.9	—
420-1	Photo-inv	0.18	1.08	0.86	1:264 000	4.6	21.4
12	Block-inv	0.30	2.01	1.70	1:200 000	2.6	—
420-1	Photo-inv	0.17	1.08	0.96	1:301 000	5.2	31.8
13	Block-inv	0.38	2.52	2.00	1:158 000	3.0	—
420-2	Photo-inv	0.18	1.65	0.95	1:274 000	5.4	34.5
14	Block-inv	0.27	1.54	1.65	1:265 000	2.0	—
420-2	Photo-inv	0.17	1.31	1.02	1:361 000	5.2	30.1
15	Block-inv	0.17	0.88	1.25	1:327 000	4.1	—
420-3	Photo-inv	0.14	0.79	1.01	1:197 000	39.4	173.0
16	Block-inv	0.16	0.74	—	1:215 000	0.4	—
420-M	Photo-inv	0.11	0.71	—	1:259 000	7.0	89.8
17	Block-inv	0.17	0.75	—	1:370 000	0.6	—
INCA-1	Photo-inv	0.17	0.78	—	1:359 000	2.4	7.0
18	Block-inv	0.18	0.84	—	1:344 000	0.6	—
INCA-2	Photo-inv	0.17	0.88	—	1:337 000	3.0	11.9

these estimates which allow a meaningful estimate of unit weight to be computed. Estimates of unit weight are not shown for the last three cases because the centroiding process used by the VMS software cannot provide a priori image measurement precisions. In these cases, the a posteriori estimate of the image measurement precision can be evaluated against prior experience. However, because the network solutions contain only equally weighted image co-ordinate observables, the a posteriori estimate is directly correlated to the r.m.s. image residual value and provides no significant extra information.

The change from block invariant to photo-invariant additional parameter models does show significant improvement in r.m.s. image residuals and the estimate of unit weight for virtually all cases in Table IV. The exceptions, cases 15, 17 and 18, are analysed further, later in this section. Numerical reductions in r.m.s. and unit weight values for the majority of cases indicate greater effectiveness of the photo-invariant model, as r.m.s. and unit weight are the prime indicators of internal network consistency. In addition, the maximum image errors are also reduced in most cases, again indicating an improved internal consistency in the networks.

Also shown in Table IV is the relative precision for the networks. With the same exceptions, virtually all cases show a significant improvement, indicating the object space precision of the network has also improved. As has been noted previously, these values may not be good indicators of relative accuracy. However, it could be expected that the change in relative precision is nevertheless a good indicator of a corresponding change in relative accuracy.

A clear disadvantage of the photo-invariant parameter model is a weakening of the networks, as compared to the block invariant model (Fraser, 1987). In all cases the relative precision, if uncorrected for the a posteriori estimate of unit weight, would be degraded in comparison to the photo-invariant model. Using case 2 as an example, if the estimates of unit weight are ignored in order to assess the affect of geometry, the uncorrected relative precision is degraded by approximately 30 per cent for the photo-invariant additional parameter set, as compared to the block invariant parameter set. The relative precisions for the networks with the block invariant and photo-invariant additional parameter models are very similar, despite the significant decrease in the r.m.s. image residual for the network using the photo-invariant model. The weakening of the network is exaggerated for case 2 because it has a relatively smaller number of targets and the target array does not have a substantial range in depth, as compared to the networks using the purpose built calibration ranges. The stronger networks show a precision degradation of no worse than 10 per cent in the uncorrected relative precisions.

This weakening of the geometric strength of the networks using the photo-invariant additional parameter model can be ascribed to:

- (a) the decrease in geometric redundancy (in the block invariant case, all photographs contribute to the determination of x_p and y_p);
- (b) an increase in the level of correlation between additional parameters from an average value of 0.15 for the block invariant case to an average value of 0.25 for the photo-invariant case (the multiple instances of x_p , for example, exhibit high correlation factors of 0.4 to 0.8); and
- (c) the small decrease in the numerical redundancy (every photograph adds two unknown parameters to the network solution).

Case 15 shows a marked degradation in relative precision for the photo-invariant case and cases 17 and 18 show a slight decrease in relative precision. These cases are exceptions to the general trend of improvement in all other cases, and the reversals are due to quite different reasons.

In case 15, the *ad hoc* target array had a depth which was slightly less than 5 per

cent of the diagonal distance across the area, severely weakening the network when combined with a relatively small number of targets and the large focal length to format ratio of the DCS420 camera with an 18 mm lens. Depth in the target array is very important in order to minimize correlations between the PP parameters and other calibration and exterior orientation parameters (Shortis and Hall, 1989). Correlations caused by projective coupling between the PP location, camera station location and camera tilts are exacerbated for a photo-invariant parameter model, because the determination of the PP parameters is individually dependent on the information contained within the image. A calibration using a block invariant parameter set and a planar target array may realize an acceptable result for the PP parameters through the use of multiple rolls, convergent images and multiple camera to object distances to minimize the coupling. However, a single photograph cannot employ these strategies and parameter dependence may lead to very strong correlations between the PP location and other parameters. In case 15, correlations approaching unity are clearly evident in the unacceptably large and unclustered variations in the PP location.

This line of reasoning is further supported by an analysis of the estimated variation of the PP co-ordinates and the actual variation in the PP co-ordinates from the photo-invariant parameter model. These data are shown in the right-hand columns of Table IV. In all cases except 15, the expected variation of the PP co-ordinates, as determined by the photogrammetric network solution, is less than 10 μm at the 99 per cent confidence limit. The actual variation in the PP position ranges from 7 μm to 90 μm . In case 15, the estimated variation is much greater at almost 40 μm and the actual variation is more than twice the maximum of all other cases, indicating that this case is an outlier which is out of character with the general trend. Reducing other cases to an almost planar array of targets showed similar, though less dramatic, results in terms of the increased correlations and PP variation.

The INCA cameras used for cases 17 and 18 are based on the Kodak Megaplug 4.2i camera, which has very different design criteria to the DCS series. This scientific camera is based on a monolithic metal casing, the CCD array is mounted in an evacuated chamber which cannot be routinely disassembled and the INCA fixed focus lens is screw mounted to the camera body. As a consequence, the Megaplug series is designed according to fundamental requirements for stability (Kodak, 1994) and indeed is widely perceived as a very stable camera. Further, there is some evidence that the INCA is significantly more stable than the DCS series (Shortis and Ganci, 1997).

In the circumstance that a camera body is stable and the CCD array is in a constant position with respect to the optical axis of the lens, little or no improvement could be expected in a calibration network due to the change from a block invariant to photo-invariant PP parameter model. Although a small amount of movement of the PP location could be expected due to the nature of the least squares estimation solution, the weakening of the network solution may realize a poorer relative precision for the photo-invariant model. This is indeed the outcome for the INCA camera calibrations, indicating that these cameras are stable and the photo-invariant model confers no significant advantage.

The expected stability of the INCA cameras was used to perform a baseline test of accuracy for the DCS420 camera. The DCS420-M, INCA-1 and INCA-2 calibration networks were captured within a few hours of one another, so that the University of Melbourne target array could be considered to be fixed. The DCS420-M data for the block invariant and photo-invariant parameter sets were then compared to the block invariant parameter sets for a combined network from the two INCA cameras. The latter network comprises 64 images, a redundancy of some 16 500 and an estimated relative precision of 1:443 000. Whilst the relative accuracy of the network

cannot be verified, the relative precision of the combined INCA network is certainly better than what could be possible with the single DCS420 camera.

Relative accuracies were computed from the r.m.s. co-ordinate difference between the co-ordinates computed from the DCS420 block invariant and photo-invariant networks and the combined INCA network. The results of the accuracy test verify that the relative accuracy of the block invariant parameter model is substantially degraded compared to the photo-invariant parameter model. The relative accuracies achieved by the DCS420-M were 1:27 000 and 1:172 000 for the block invariant and photo-invariant cases, respectively. It is no surprise that the relative accuracy for the photo-invariant parameter set case is poorer than the relative precision by a factor of approximately 1.5. However, the factor of eight for the block invariant parameter set case is unexpected. A degradation by a factor of eight is an extreme disparity between the relative precision and relative accuracy. Further, the block invariant case showed clear systematic trends in the co-ordinate differences, whilst the photo-invariant case showed a primarily random pattern of error such as that shown in Fig. 4.

It must be stressed here that this isolated case is probably exceptional, as prior research has shown that the discrepancy between relative precision and relative accuracy has been verified at lower levels (Fraser and Shortis, 1995). It could be expected that the degree of degradation would depend on the inherent stability of the camera in terms of the variation of the PP location, and this behaviour is investigated in the next section.

BEHAVIOUR OF THE PP LOCATION

The behaviour of the PP location is conveniently analysed using plots of the position within the image co-ordinate system. The position plots are based on the PP locations produced by the photo-invariant additional parameter model for individual exposures and the single PP location for all exposures produced by the block invariant additional parameter model. For the sake of consistency, only the cardinal roll angle locations of the photo-invariant PP are shown on each plot. In order to identify clustering, common symbols are used for PP locations derived from exposures with approximately the same cardinal roll angles. In all cases the units of the position locations are millimetres.

Comparison of cases 1 and 2 in Fig. 6 demonstrates clearly the varied behaviour of different cameras. Here the lens was identical and the calibration scenario was very similar, yet the location and range of variation of the PP within the image is quite different. In neither case is there any clustering apparent, indicating that the random rolling of the camera prevents any consistency in the relocation of the CCD array for any particular roll angle.

A much clearer clustering of PP positions is shown in Fig. 7. In these cases, a dual roll strategy was used, which comprised two exposures at each station in the regular order of 0° and 90°. In cases 3 and 4, the same camera was used with the calibration field but with two different lenses. Different general locations could be expected and this is realized. However, a similar pattern of PP locations would be expected and this is not so. Whilst the scatter of the PP for each cardinal roll angle is similar, especially in the x axis direction, the relative positions of the two clusters are not similar. The confounding factor here may be that the two calibrations were separated by approximately one month during which the camera was used for project work.

The four cases of quadruple roll strategy for camera DCS460-2 shown in Fig. 8 present both explainable and unexplainable behaviour. All four cases used the calibration field, 32 exposures and a similar layout of eight camera stations. Cases 5

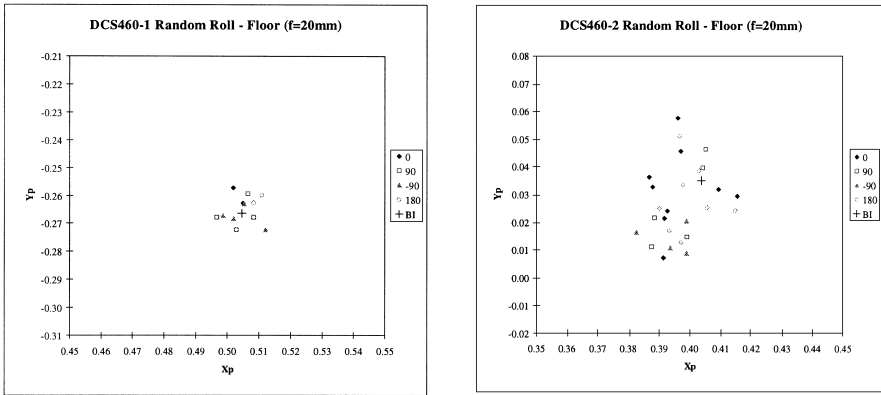


FIG. 6. Principal point location variations (mm) for cases 1 and 2.

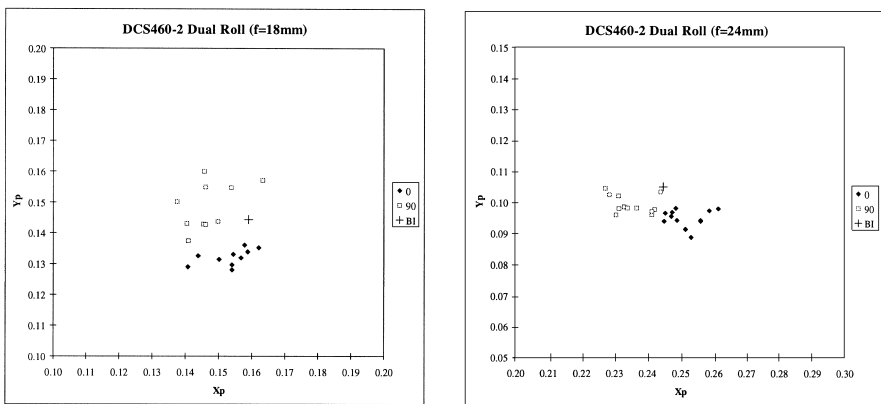


FIG. 7. PP location variations (mm) for cases 3 and 4.

and 6, shown on the top row, used a quadruple roll strategy where four exposures were taken at each camera station in no particular order. For case 6, the camera was shaken before every exposure to simulate rough handling. The greater spread of PP locations for case 6 is clear evidence that handling of the camera does have an influence on the CCD array position. Cases 7 and 8, shown on the bottom row, used a consistent quadruple roll strategy where every camera station was visited four times with the camera held in a cardinal roll position throughout each pass around the camera stations. The clearly evident clustering is proof that the CCD array does take up a stable location within the focal plane. The left-hand column in Fig. 8, cases 5 and 7, used the same lens. The block invariant PP location and the extent of the photo-invariant locations are comparable, with the more evident clustering in case 7 explainable due to the consistent roll.

Case 8, on the bottom right of Fig. 8, shows extremely clear and symmetrical clustering and there is a strong correlation between this behaviour and the predicted behaviour of the PP location shown in Fig. 2. However, cases 7 and 8 on the bottom row of Fig. 8 could be expected to show similar behaviour and clearly do not. Again,

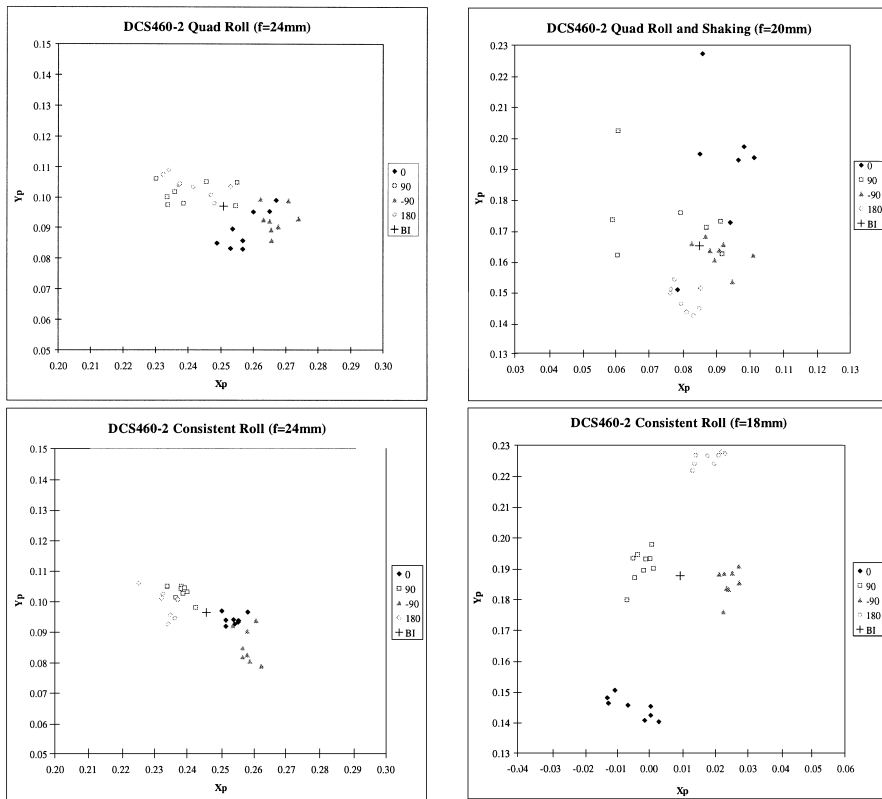


FIG. 8. PP location variations (mm) for cases 5 (top left), 6 (top right), 7 (bottom left) and 8 (bottom right).

the confounding factor may be the time delay of several days between cases 7 and 8, during which time the camera was involved in project work. In contrast, the calibrations for cases 5 and 7 were conducted on the same day.

The simple act of changing lenses may have the potential to contribute to the unexplained behaviour. The pressure on the lens mount and twisting motion of removal and insertion may affect the configuration of the camera body and digital back, in turn changing the pressure on the CCD array mount. As has been previously stated, the looseness of the CCD array is very dependent on the mechanical relationship between the camera body and digital back.

The third DCS460 camera tested was opportunistically calibrated using a consistent roll strategy and the PP location variation shown in Fig. 9 again indicates strong clustering. This calibration was curtailed by a miscalculation of the available space on the PCMCIA disk drive and, as a result, the exposures for only the first three rolls were completed. Despite this, the clustering again has a striking correlation with the predicted movement in Fig. 2 and the position of the block invariant PP is in good agreement with the expected physical model.

Shown in Fig. 10 is a comparison of two DCS420 cameras calibrated under very similar circumstances. The fundamental difference between these two cameras was that DCS420-1 is the camera shown in Fig. 5, which was stabilized by clamping the

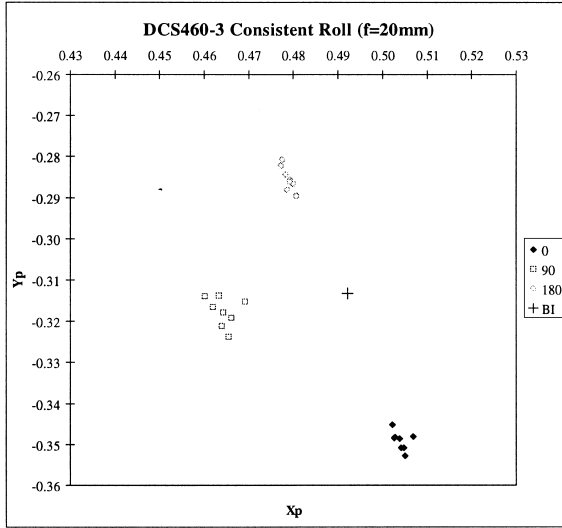


FIG. 9. PP location variations (mm) for case 9.

camera body to the digital back and partially fixing the CCD array to the digital back (Shortis and Beyer, 1997). The change in behaviour of DCS420-1, whilst not prominent, is apparent. The spread of the PP locations is less and there is some evidence of clustering for DCS420-1, whilst DCS420-2 shows a very random pattern of PP locations. As previously noted, whilst the camera modification was impractical, the improvement in calibration stability was significant. The reduction in the PP variation demonstrated here is also significant, but probably insufficient to justify the modification as a viable alternative to the photo-invariant solution even if a practical stabilization mechanism could be contrived.

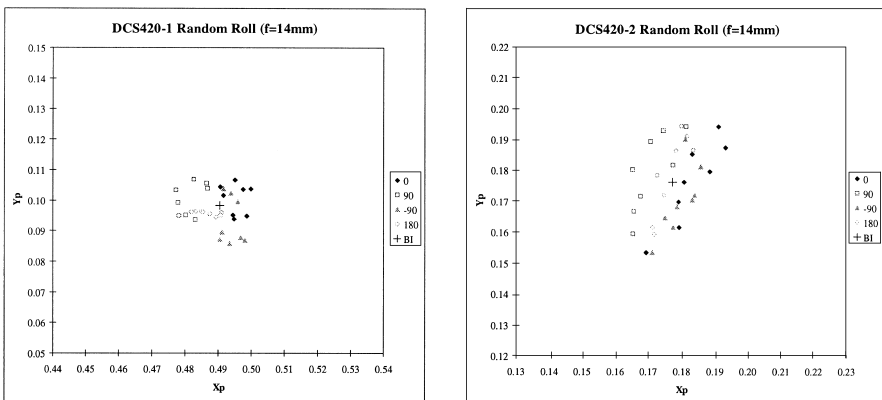


FIG. 10. PP location variations (mm) for cases 11 and 13.

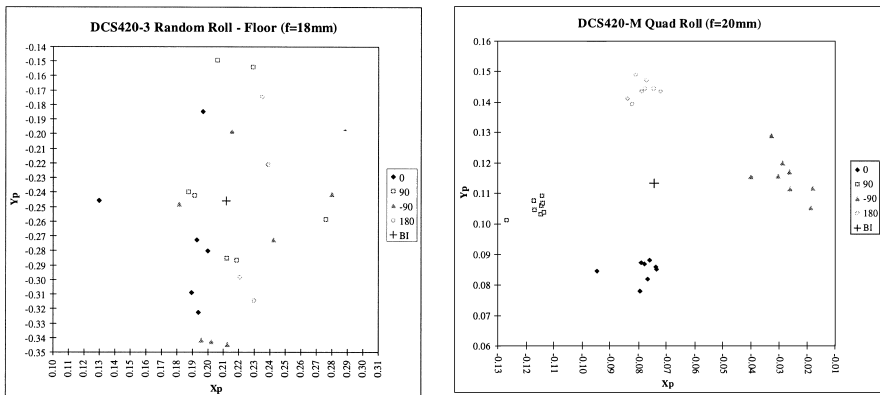


FIG. 11. PP location variations (mm) for cases 15 and 16.

Fig. 11 shows a further two cases of DCS420 camera calibrations. The left-hand chart shows the single result for the DCS420–3 camera. The very large variation (note that the extent of this chart is more than twice that of the other charts) shown here is not considered to be physical movement, but instead is a phenomenon associated with a weak network as discussed in the previous section. In contrast, the right-hand chart shows the result for the University of Melbourne DCS420 with a very strong network and demonstrates very clear clustering of the PP locations for each of the four roll angles, despite the fact that this was not a case of consistent roll handling.

The results for the two INCA cameras are shown in Fig. 12. As could be expected, the variation in the PP location is much less because the Megaplus series has a very different design, which has greater inherent stability. There is a clear difference in results for the two cameras, as INCA-1 shows a much tighter grouping of PP locations around the block invariant location, indicating that this camera is more stable. Considering that the method and circumstances of the calibration were virtually identical for the two cameras, this result shows that there is also some variation in the behaviour of this type of high resolution, scientific camera.

Variation in behaviour is clearly demonstrated for the DCS cameras, as could be inferred from the camera design and construction. Whilst the cases of consistent roll strategy provide evidence that the behaviour can be modified by careful handling, the wide variety of PP location variation and patterns of clustering for the “typical use” cases indicates that every camera may be different. Indeed, the behaviour of the camera in terms of the PP location seems also to be modified by time or use in between calibrations. Such variation is contrary to the development of a generic the predicted movement in Fig. 2 and the position of the block invariant PP is in good agreement with the expected physical model.

Shown in Fig. 10 is a comparison of two DCS420 cameras calibrated under very similar circumstances. The fundamental difference between these two cameras was that DCS420–1 is the camera shown in Fig. 5, which was stabilized by clamping the physical model, other than the photo-invariant PP parameter model.

BLOCK INVARIANT VERSUS OTHER PP MODELS

Despite the generally random behaviour of the typical use cases for the DCS cameras, the two additional photo-invariant models proposed earlier in the paper were tested with some of the first 16 cases in Table IV. A subset of cases was selected to

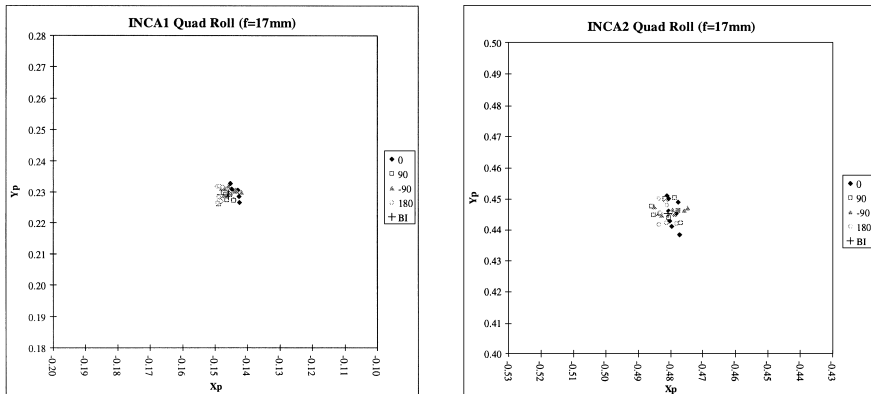


FIG. 12. PP location variations (mm) for cases 17 and 18.

illustrate the full range of roll strategies for typical use of the DCS460 and DCS420 cameras. Cases of consistent roll were excluded on the basis that these are not typical use scenarios and therefore may be misleading in terms of the effectiveness of the two additional parameter models tested.

The results shown in Table V indicate that, in general, the elliptical motion and roll clustered photo-invariant PP additional parameter models are not effective. Whilst, in most cases, there is a reduction in the r.m.s. image residual, indicating an improved level of internal consistency for the networks, this is not translated into significant improvements in relative precision due to the weakening of the networks as previously discussed. In cases such as 2 and 13, the relative precision is degraded, rather than maintained or improved. The lack of effectiveness is due to the meagre level of clustering of the PP locations in most cases. Cases 2 and 13, in particular, show a very random pattern of PP locations, which is quite contrary to the expectation of the two additional parameter models.

The exception to this is case 16, which does indicate an improvement in both the r.m.s. image residuals and the relative precisions for the elliptical motion and roll clustered photo-invariant PP additional parameter models. The evident clustering of PP locations for this camera is in accord with the fundamental assumptions of the two models, leading to a significant reduction in systematic error and a consequent improvement in internal consistency which is over and above the weakening of the geometric strength of the network. However, it should be noted that, like all other cases, the independent photo-invariant PP additional parameter model exhibits the most internally consistent and precise network.

CONCLUSIONS

This investigation has shown that PP movement in the DCS series of cameras is a real phenomenon, which does degrade the integrity of self calibrating networks. Although other effects which contribute to the instability of the camera may be present, the response of the CCD array to camera roll is the most evident source of systematic error. The magnitude of the effect varies between cameras, which is most probably correlated with the stiffness of the spring mounting of the CCD array and the pressure on the surround of the array when the camera body is attached to the digital back. There is also some indication that the same camera can vary in behaviour due to disassembly and, perhaps, due to routine use.

TABLE V. Results for the selected calibration data sets used in the experimental testing.

<i>Case and camera</i>	<i>Additional parameter model</i>	<i>R.m.s. image error (μm)</i>	<i>Maximum image error (μm)</i>	<i>Estimate of unit weight</i>	<i>Estimated relative precision</i>
2	Block invariant	0.42	3.24	3.19	1:268 000
Random	Elliptical motion PP	0.42	3.22	3.19	1:260 000
Roll	Roll clustered PP	0.41	3.24	3.13	1:260 000
460-2	Photo-invariant PP	0.20	2.80	2.23	1:271 000
3	Block invariant	0.44	3.25	1.96	1:183 000
Dual	Elliptical motion PP	0.40	4.20	1.78	1:192 000
Roll	Roll clustered PP	0.40	4.17	1.80	1:190 000
460-2	Photo-invariant PP	0.20	2.80	0.98	1:359 000
5	Block invariant	0.39	2.88	1.47	1:279 000
Quad	Elliptical motion PP	0.38	2.71	1.44	1:281 000
Roll	Roll clustered PP	0.32	2.80	1.23	1:322 000
460-2	Photo-invariant PP	0.25	2.69	0.95	1:360 000
6	Block invariant	0.76	6.42	3.09	1:138 000
Quad	Elliptical motion PP	0.65	5.43	2.68	1:158 000
Shaken	Roll clustered PP	0.62	6.18	2.56	1:162 000
460-2	Photo-invariant PP	0.29	2.30	1.15	1:333 000
13	Block invariant	0.38	2.52	2.00	1:158 000
Quad	Elliptical motion PP	0.40	4.33	2.12	1:144 000
Roll	Roll clustered PP	0.38	4.40	2.03	1:145 000
420-2	Photo-invariant PP	0.18	1.65	0.95	1:274 000
16	Block invariant	0.16	0.74	—	1:215 000
Quad	Elliptical motion PP	0.14	0.69	—	1:228 000
Roll	Roll clustered PP	0.13	0.77	—	1:238 000
420-M	Photo-invariant PP	0.11	0.71	—	1:259 000

The most general and effective solution is the independent photo-invariant PP additional parameter model, which assigns a different PP location to every exposure. This solution does not rely on a physical model of the CCD array movement within the focal plane. The disadvantage of this solution is an inherent weakening of the photogrammetric network. However, this is of little consequence in comparison to the improvement in the internal consistency of the network. Further, the majority of industrial metrology applications employ many exposures, due to the available image capacity of the DCS cameras, which realizes a very high level of reliability and overcomes the effect of the increased number of unknown parameters.

The elliptical motion and roll clustered photo-invariant PP additional parameter models are based on an analysis of the physical cause of the systematic changes in the PP location with roll angle, but these models are ineffective in most cases. The ineffectiveness is due to the random nature of the PP locations, as shown in the behaviour analysis based on the independent photo-invariant additional parameter model. The magnitude and randomness of the PP location patterns vary from camera to camera. However, none of the cameras tested in a typical use regime exhibited sufficient consistency for these models to be as effective as the independent photo-invariant additional parameter model.

Although the independent photo-invariant additional parameter model does successfully model the systematic error in the DCS series cameras, a better solution is to design and/or use a stable camera system, such as the Megaplug series, for high precision vision metrology. Use of an extended calibration algorithm, no matter how effective, will always be a compromise because it cannot be universal. There will always be circumstances where such a solution will fail, such as near planar target

arrays, small numbers of targets, small numbers of images or a combination of all of these factors. However, if Kodak DCS series cameras are used with the independent photo-invariant additional parameter model and very strong self calibrating photogrammetric networks, significantly improved relative precisions and accuracies can be achieved.

REFERENCES

- BEYER, H. A., 1995. Digital photogrammetry in industrial applications. *International Archives of Photogrammetry and Remote Sensing*, 30(5W1): 373–378.
- DOLD, J., 1996. Influence of large targets on the results of photogrammetric bundle adjustment. *Ibid.*, 31(B5): 119–123.
- FRASER, C. S., 1987. Multiple exposures in non-metric camera applications. *Photogrammetria*, 42(1/2): 62–72.
- FRASER, C. S., 1997. Innovations in automation for vision metrology systems. *Photogrammetric Record*, 15(90): 901–911.
- FRASER, C. S. and SHORTIS, M. R., 1992. Variation of distortion within the photographic field. *Photogrammetric Engineering & Remote Sensing*, 58(6): 851–855.
- FRASER, C. S. and SHORTIS, M. R., 1995. Metric exploitation of still video imagery. *Photogrammetric Record*, 15(85): 107–122.
- FRASER, C. S., SHORTIS, M. R. and GANCI, G., 1995. Multi-sensor system self-calibration. *Videometrics IV*. SPIE 2598: 2–18.
- FRYER, J. G., 1985. Non-metric photogrammetry and surveyors. *Australian Surveyor*, 32(5): 330–341.
- FRYER, J. G., 1996. Camera calibration. *Close range photogrammetry and machine vision* (Ed. K. B. Atkinson). Whittles Publishing, Caithness. 371 pages: 156–179.
- GRUEN, A., MAAS, H.-G. and KELLER, A., 1995. Kodak DCS200—a camera for high accuracy measurements? *Videometrics IV*. SPIE 2598: 52–59.
- KENEFICK, J. F., GYER, M. S. and HARP, B. F., 1972. Analytical self calibration. *Photogrammetric Engineering*, 38(11): 1117–1126.
- KODAK, 1994. *Kodak Megaplug Camera, Model 1.4, expanded specification revision A*. Motion Analysis Systems Division, Eastman Kodak Company, Rochester, New York. 35 pages.
- LUHMANN, T., 1996. Results of the German comparison test for digital point operators. *International Archives of Photogrammetry and Remote Sensing*, 31(B5): 324–329.
- MAAS, H.-G. and NIEDERÖST, M., 1997. The accuracy potential of large format still video cameras. *Videometrics V*. SPIE 3174: 145–152.
- MILLS, J. P., NEWTON, I. and GRAHAM, R. W., 1996. Aerial photography for survey purposes with a high resolution, small format, digital camera. *Photogrammetric Record*, 15(88): 575–587.
- PEIPE, J., 1995. Photogrammetric investigation of a 3000 × 2000 pixel high resolution still video camera. *International Archives of Photogrammetry and Remote Sensing*, 30(5W1): 36–39.
- PEIPE, J., 1997. High-resolution CCD area array sensors in digital close range photogrammetry. *Videometrics V*. SPIE 3174: 153–156.
- PETRAN, F., KRZYSZEK, P. and BONITZ, P., 1996. CAD-based reverse engineering with digital photogrammetry. *International Archives of Photogrammetry and Remote Sensing*, 31(B5): 475–480.
- ROBSON, S. and SHORTIS, M. R., 1998. Practical influences of geometric and radiometric image quality provided by different digital camera systems. *Photogrammetric Record*, 16(92): 225–248.
- SHORTIS, M. R. and HALL, C. J., 1989. Network design methods for close-range photogrammetry. *Australian Journal of Geodesy, Photogrammetry and Surveying*, 50: 51–72.
- SHORTIS, M. R. and BEYER, H. A., 1996. Sensor technology for digital photogrammetry and machine vision. *Close range photogrammetry and machine vision* (Ed. K. B. Atkinson). Whittles Publishing, Caithness. 371 pages: 106–155.
- SHORTIS, M. R. and BEYER, H. A., 1997. Calibration stability of the Kodak DCS420 and 460 cameras. *Videometrics V*. SPIE 3174: 94–105.
- SHORTIS, M. R. and GANCI, G., 1997. Calibration stability of digital still cameras for industrial inspection. *International Conference on Measurement Science, Technology and Practice*, Melbourne, Australia. Pages: 245–250.
- SHORTIS, M. R., CLARKE, T. A. and ROBSON, S., 1995. Practical testing of the precision and accuracy of target image centring algorithms. *Videometrics IV*. SPIE 2598: 65–76.
- SHORTIS, M. R., ROBSON, S. and SHORT, T., 1996. Multiple focus calibration of a still video camera. *International Archives of Photogrammetry and Remote Sensing*, 31(B5): 534–539.
- STREILEIN, A. and GASCHEN, S., 1994. Comparison of a S-VHS camcorder and a high-resolution CCD-camera for use in architectural photogrammetry. *Ibid.*, 30(5): 382–389.
- SUSSTRUNK, S. and HOLM, J., 1995. Camera data sheet for pictorial electronic still cameras. *Cameras and Systems for Electronic Photography and Scientific Imaging*. SPIE 2416: 5–16.
- TRINDER, J. C., 1989. Precision of digital target location. *Photogrammetric Engineering & Remote Sensing*, 55(6): 883–886.

Résumé

On a largement adopté les caméras numériques dans les applications de photogrammétrie à courte distance et de vision robotique. Etant données les avantages de l'enregistrement sur place des images numériques, la facilité et la rapidité du traitement des données, les caméras numériques sont devenues rapidement un équipement standard pour les travaux de mesures en métrologie industrielle et pour enregistrer les données du patrimoine. Comme dans toute application métrique, la précision que l'on peut obtenir sur les objets dépend, entre autres, de la précision de l'étalonnage de la caméra. Dans la grande majorité des applications photogrammétriques il suffit d'utiliser un modèle d'étalonnage invariant dans le bloc, définissant les paramètres physiques élémentaires, et notamment la position du point principal. Mais dans le cas des caméras Kodak DCS 420 et DCS 460, conçues pour un usage domestique et les reportages photographiques, on sait très bien que cet étalonnage est instable du fait de leur réalisation, basée sur le corps d'une caméra SLR 35 mm. En particulier, des études antérieures ont montré que la position du point principal était sujette à des déplacements pendant la manipulation normale de la caméra, provoqués par le dispositif de montage de la matrice des DTC (CCD). On décrit dans cet article une recherche menée sur la tenue physique de la position du point principal et l'on compare différents modèles des paramètres d'étalonnage des caméras numériques Kodak DCS 420 et DCS 460.

Zusammenfassung

Digitale Standkameras werden weitverbreitet für Anwendungen in der Nahphotogrammetrie und beim Maschinensehen adoptiert. Wegen der Vorteile der Speicherung der digitalen Bilder in der Kamera und der schnellen Datenverarbeitung werden digitale Standkameras rasch zur Standardausrüstung für Meßaufgaben, wie z.B. die industrielle Metrologie und die Aufzeichnung des kulturellen Erbes. Wie für jede metrische Anwendung hängt die Genauigkeit der abgeleiteten Objektdaten neben vielen anderen Faktoren von der Genauigkeit Kammerkalibrierung ab. Für die meisten photogrammetrischen Anwendungen ist die Nutzung des einfachen Falls eines blockinvarianten Kalibrierungsmodells, das die hauptsächlichsten physikalischen Parameter einschließlich der Lage des Hauptpunktes umfaßt, ausreichend. Kameras, die jedoch für Bildjournalisten und häuslichen Gebrauch konstruiert wurden, wie z.B. die Kameras DCS420 und DCS640 von Kodak, sind für ihre Kalibrierungsinstabilität gut bekannt, weil ihre Konstruktion auf dem Kamerakörper einer 35 mm SLR-Kamera beruht. Insbesondere hat vorhergehende Forschung ergeben, daß die Lage des Hauptpunktes während der normalen Kamerabehandlung zur Bewegung neigt, und zwar wegen der Mechanik, wie die CCD-Matrix befestigt ist. Im Beitrag wird über eine Untersuchung des physikalischen Verhaltens der Lage des Bildhauptpunktes berichtet, und es werden verschiedene Kalibrierungsparameter-Modelle für die Standkameras DCS420 und DCS640 von Kodak verglichen.